Comunicações Geológicas

Comunicações Geológicas (2025) 112, Especial I, 29-33
ISSN: 0873-948X; **e-ISSN**: 1647-581X

Compositional heterogeneity of late to post-Variscan, mafic subvolcanic dykes from northern Portugal (Central Iberian Zone)

Heterogeneidade composicional dos ciques máficos subvulcânicos, tardi a pós-variscos do norte de Portugal (Zona Centro Ibérica)

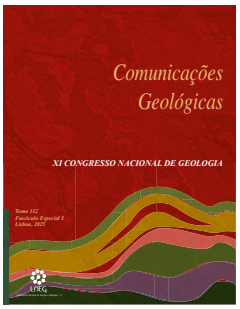

A. J. T. Oliveira[1,2*] , H. C. B. Martins[1,2] , H. Sant'Ovaia[1,2]

DOI: https://doi.org/10.34637/7dm2-f386
Recebido em 01/10/2023 / Aceite em 08/01/2024
Publicado online em abril de 2025

Artigo original
Original article

Abstract: This study is dedicated to the presentation and interpretation of whole-rock geochemical data concerning a few mafic subvolcanic dykes located in northern Portugal, related to the late to post-tectonic stages of the Variscan orogeny. Overall, the analyzed rocks are reasonably fresh, ultrabasic to intermediate, metaluminous to moderately peraluminous, and calc-alkaline or alkaline. There is no evidence implying the occurrence of crustal contamination, but crystal fractionation is likely to have played either a minor or more meaningful role on the petrogenetic evolution. While most dykes were probably generated from subduction-modified, metasomatically-enriched lithospheric sources, others possibly derived from the asthenosphere. There are also important differences regarding the residual mineralogy of the sources, as well as the melting degrees.

Keywords: Lamprophyres, Dolerites, Dykes, Permo-Carboniferous Magmatism, Variscan Orogeny.

Resumo: O presente trabalho dedica-se à apresentação e interpretação de dados de geoquímica de rocha total sobre alguns diques subvulcânicos máficos, localizados no norte de Portugal, associados às fases tardi a pós-tectónicas da orogenia Varisca. Em geral, as rochas analisadas são razoavelmente frescas, ultrabásicas a intermédias, metaluminosas a moderadamente peraluminosas, e calcoalcalinas ou alcalinas. Não existem evidências a favor da ocorrência de contaminação crustal, mas a cristalização fracionada deverá ter desempenhado um papel mais ou menos significativo sobre a evolução petrogenética. Embora a maioria dos diques tenha provavelmente sido gerada a partir de fontes litosféricas, modificadas por subducção e enriquecidas metassomaticamente, os restantes possivelmente derivaram da astenosfera. Existem ainda diferenças importantes no que diz respeito à mineralogia residual das fontes, assim como sobre os respetivos graus de fusão.

Palavras-chave: Lamprófiros, Doleritos, Diques, Magmatismo Permo-carbonífero, Orogenia Varisca.

1. Introduction

The Permo-Carboniferous hypabyssal magmatism is a widespread igneous event throughout NW and SW Europe, related to the post-collisional setting that followed the Variscan orogeny. The aforementioned magmatic episode was brought upon by the reorganization of the stress field in Europe, at that time, due to the transition from a compressive/transpressive to extensional/transtensive setting (*e.g.*, Kirstein *et al.*, 2006; Soder and Romer, 2018). The generation of late to post-Variscan subvolcanic rocks in Iberia, as well as in both central and western Europe, has thus been associated with the onset of intracontinental rifting, implicating lithospheric thinning, passive upwelling of the hot asthenospheric mantle, and melting forced by adiabatic decompression (Perini *et al.*, 2004; Orejana *et al.*, 2008, 2020; Villaseca *et al.*, 2022). In western Armorica, the asthenospheric upwelling is suggested to have been caused by extension related to roll-back of the subducted lithospheric plate or delamination of the deep part of the overlying lithospheric mantle (Caroff *et al.*, 2021). In northern Portugal, the Permo-Carboniferous magmatism is materialized in numerous dykes, sills, and masses of hypabyssal lithologies such as porphyries, microgranites, lamprophyres, and dolerites. Even though the existence of these lithotypes has been recognized since the 20th century (*e.g.*, Ferreira and Macedo, 1979), due to the highly advanced alteration, their petrographic and geochemical features have only been poorly constrained. This work reports the bulk-rock composition of some reasonably fresh, late to post-Variscan, mafic dykes found in northern Portugal, and provides a few insights into their petrogenesis.

2. Geological Setting

The dykes analyzed within the compass of this work are located in five different regions of northern Portugal (Figura 1). The studied specimens include the Lamas de Olo (LO) lamprophyre (classified as a minette; Oliveira *et al.*, 2022), a microgabbro from Vila Nova de Foz Côa (VNFC), and several dolerites from the Vila Real (VR), Penafiel, and Torre de Moncorvo (TM) regions. Even though most dykes are relatively small (for instance, the LO lamprophyre is only ca. 300 m long and 0.3 to 0.4 m wide), others (like the TM dolerites) define alignments, at most 7.5 km long. They are also hosted in syn, late, or post-Variscan granites, as well as in metasedimentary units of the Douro Group. The contacts between the hypabyssal and host rocks are always sharp. Moreover, the subvolcanic mafic dykes are emplaced

[1] Faculdade de Ciências da Universidade do Porto, Departamento de Geociências, Ambiente e Ordenamento do Território, Rua do Campo Alegre, s/n, 4169-007 Porto, Portugal.

[2] Instituto de Ciências da Terra, Polo do Porto, Rua do Campo Alegre, s/n, 4169-007 Porto, Portugal.

* Corresponding author / Autor correspondente: up201107754@edu.fc.up.pt

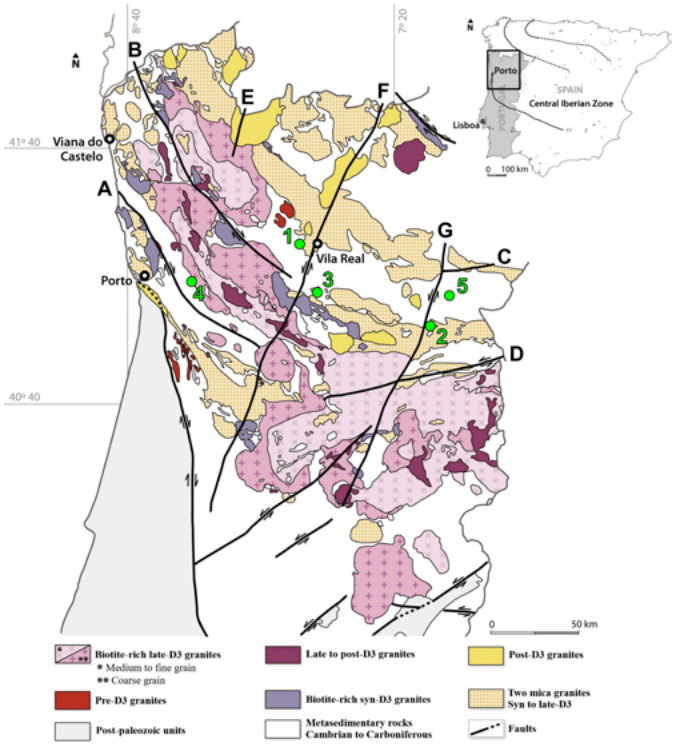

Figure 1. Simplified geological map of northern Portugal (adapted from Ferreira *et al*., 1987) and respective legend. Geologic structures: A – Dúrico-Beirão Carboniferous Trough shear zone; B – Vigo-Régua shear zone; C – Moncorvo-Bemposta shear zone; D – Traguntia-Penalva do Castelo shear zone; E – Gerês-Lovios fault; F – Penacova-Régua-Verin fault; G – Vilariça fault. Study areas: 1 – Lamas de Olo; 2 – Vila Nova de Foz Côa; 3 – Vila Real; 4 – Penafiel; 5 – Torre de Moncorvo.

Figura 1. Mapa geológico simplificado do norte de Portugal (adaptado de Ferreira et al., 1987) e respetiva legenda. Estruturas geológicas: A – Zona de cisalhamento do Sulco Carbonífero Dúrico-Beirão; B – Zona de cisalhamento Vigo-Régua; C – Zona de cisalhamento Moncorvo-Bemposta; D – Zona de cisalhamento Traguntia-Penalva do Castelo; E – Falha Gerês-Lovios; F – Falha Penacova-Régua-Verin; G – Falha da Vilariça. Áreas de estudo: 1 – Lamas de Olo; 2 – Vila Nova de Foz Côa; 3 – Vila Real; 4 – Penafiel; 5 – Torre de Moncorvo.

along late to post-D_3 structures, which are dominantly E-W, NE-SW, or NW-SE trending. For comparative purposes, two additional specimens of an alkali basalt dyke found in Gonçalo (Guarda), originally studied by Ramos and Noronha (2019), were also taken into account. This lithotype is mineralogically and geochemically identical to the VNFC microgabbro.

3. Petrography

Overall, the mafic lithologies are essentially composed of biotite, clinopyroxene (diopside and augite), K-feldspar, plagioclase (labradorite-bytownite), and amphibole (tremolite-actinolite and magnesiohornblende), while quartz, magnetite, ilmenite, apatite, orthopyroxene (enstatite), olivine, zircon, monazite, calcite, chlorite, hematite/goethite, muscovite, and serpentine constitute accessory phases. The LO lamprophyre displays a typical porphyritic texture, the dolerites are phaneritic and fine to medium-grained, and the VNFC microgabbro presents an aphyric, microcrystalline texture. Other interesting textural features include quartz xenocrysts in the LO lamprophyre, monocrystalline and polycrystalline quartz ocelli in the TM dolerites, as well as calcite and chlorite ocelli in the VNFC microgabbro. Furthermore, all dolerites reveal common subophitic and intergranular textures.

4. Methodologies

For this study, eighteen samples were used: three from the LO lamprophyre, one of the VNFC microgabbro, three from the VR dolerite, one representing the Penafiel dolerite, and the remaining ten from the TM dolerites. Bulk-rock analyses for lithogeochemical purposes were conducted at the Activation Laboratories in Ancaster (Ontario, Canada) based on the WRA + trace 4Litho analytical package protocol. Samples were fused in a solution of lithium metaborate and tetraborate, subsequently analyzed by ICP (Inductively Coupled Plasma) and ICP/MS (Inductively Coupled Plasma/Mass Spectrometry), diluted, and analyzed once more by a Perkin Elmer Sciex ELAN 6000, 6100, or 9000 ICP/MS equipment. For each sample, mass analysis was required as an additional quality control technique, where totals should vary between 98.5% and 101%. The following are the respective detection limits: (i) 0.01% for major elements (Al_2O , CaO, $Fe_2O_3^T$, K_2O, MgO, Na_2O, P_2O_5, and SiO_2); (ii) 0.001% for minor elements (MnO and TiO_2); and (iii) 0.01–30 ppm for trace elements. Precision is 1–2% (for major and minor elements) or 20% (for trace elements) at greater than 100 times the detection limit.

Two additional methods were employed to determine Li and F contents namely sodium peroxide fusion (following the 8-Peroxide-ICPMS analytical protocol) and a technique based on an Ion Selective Electrode (code 4F-F-ISE), respectively. The former analysis required an initial sodium peroxide fusion, followed by acid dissolution. Samples were then analyzed by the Perkin Elmer Sciex ELAN 6000, 6100, or 9000 ICP/MS equipment. The corresponding detection limit is 0.001%. On the other hand, to measure F concentrations, samples were fused with a mixture of lithium metaborate and tetraborate in an induction furnace to release fluoride ions from the sample matrix. Afterward, the fuseate was dissolved in dilute nitric acid, the resulting solution complexed, and the ionic strength adjusted with an ammonium citrate buffer. Finally, a fluoride ion electrode was immersed in the final solution to measure the fluoride-ion activity directly. An automated fluoride analyzer (Mandel Scientific) was used for the analysis. The associated detection limit is 0.01%.

5. Results

All specimens exhibit high LOI values (3.05–7.68%). For the LO lamprophyre, this feature is primary and related to the characteristic high volatile contents and corresponding elevated proportions of composing hydrous minerals such as biotite and amphibole (Rock, 1991). For the VNFC microgabbro, Penafiel dolerite, and Gonçalo samples, the major and trace element concentrations (namely high CaO, higher Na_2O compared to K_2O, and low Ba and Rb) suggest that alteration was not significant, meaning that both LILE and HFSE provide primary information about the petrogenesis. On the other hand, taking into account the reasonable correlations between LOI values and some mobile elements (like $Fe_2O_3^T$, P_2O_5, CaO, Na_2O, Ba, Rb, Sr, and F) for the LO lamprophyre and VR plus TM dolerites, it is plausible to presume that the post-magmatic alterations which influenced these rocks were only moderately significant, having mainly disturbed the contents of the most mobile elements.

Considering the SiO_2 concentrations, the LO lamprophyre and VR dolerite are chemically intermediate, the TM dolerites are basic to intermediate, the Penafiel and Gonçalo specimens are basic, and the VNFC microgabbro is ultrabasic. Furthermore, the microgabbro is presumably the most primitive rock (#Mg = 0.65), whereas the VR dolerite is probably the most evolved one (#Mg = 0.54–0.56). The LO lamprophyre is ultrapotassic, calc-alkaline to alkaline, and weakly to moderately peraluminous, the VR and TM dolerites are calc-alkaline and metaluminous to weakly peraluminous, the VNFC microgabbro

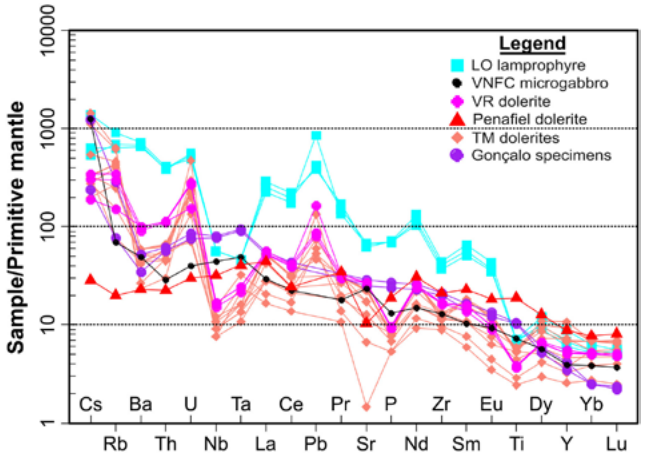

Figure 2. Multi-element spidergrams for the mafic subvolcanic dykes. Primitive mantle normalization values after McDonough and Sun (1995).

Figura 2. Diagramas multielementares dos diques máficos subvulcânicos, normalizados tendo em conta a composição do manto primitivo de McDonough and Sun (1995).

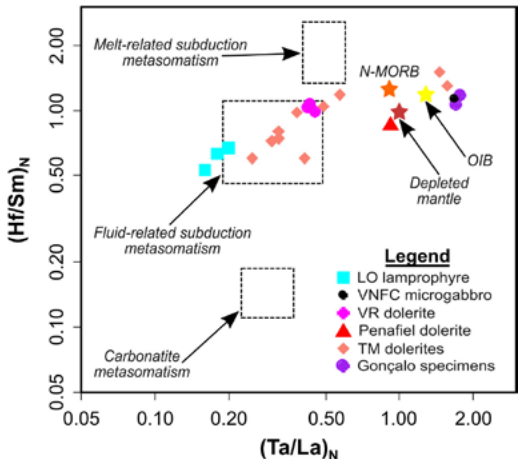

Figure 4. Projection of the mafic hypabyssal dykes in the $(Ta/La)_N$ versus $(Hf/Sm)_N$ binary diagram. Fields representing distinct metasomatic components after LaFlèche et al. (1988).

Figura 4. Projeção dos diques máficos hipabissais no diagrama binário $(Ta/La)_N$ versus $(Hf/Sm)_N$. Os campos representativos das várias componentes metassomáticas foram adaptados de LaFlèche et al. (1988).

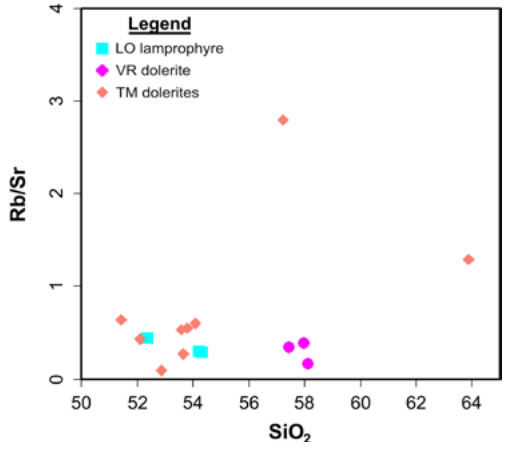

Figure 3. Projection of the Lamas de Olo lamprophyre, Vila Real and Torre de Moncorvo dolerites in the SiO_2 versus Rb/Sr binary diagram.

Figura 3. Projeção do lamprófiro de Lamas de Olo e dos doleritos de Vila Real e Torre de Moncorvo no diagrama binário SiO_2 versus Rb/Sr.

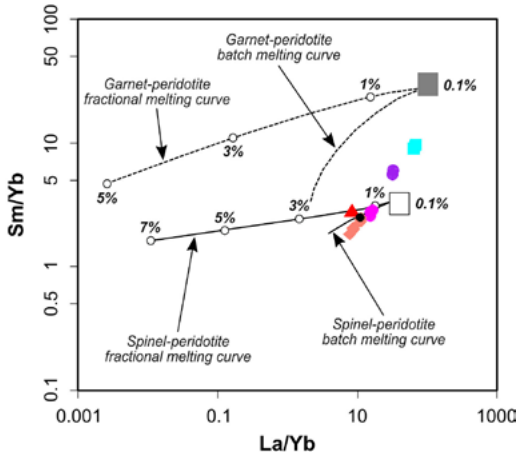

Figure 5. Projection of the mafic subvolcanic dykes in the La/Yb versus Sm/Yb binary diagram. The grey and white fields respectively represent the starting compositions of garnet and spinel-bearing peridotites at a 0.1% melting degree (Alici Şen et al., 2004). Melting curves were obtained from the equations of Shaw (1970). Garnet and spinel-peridotite compositions are from Sen and Leeman (1991) and McDonough (1990). Legend as in figure 2.

Figura 5. Projeção dos diques máficos subvulcânicos no diagrama binário La/Yb versus Sm/Yb. Os campos cinzento e branco representam, respetivamente, as composições iniciais de peridotitos ricos em granada e espinela sob um grau de fusão de 0.1% (Alici Şen et al., 2004). As curvas de fusão foram obtidas a partir das equações de Shaw (1970). As composições dos peridotitos ricos em granada e espinela são as publicadas por Sen and Leeman (1991) e McDonough (1990). Legenda como na figura 2.

and Gonçalo specimens are alkaline and metaluminous, and the Penafiel dolerite is metaluminous and presents both alkaline and tholeiitic features (Nb/Y = 0.55; Zr/Nb = 10.57). Moreover, the lamprophyre is remarkably enriched in K_2O, Ba, Sr, Sn, W, and REE, when compared to all other dykes. Based on geotectonic classifications, even though these subvolcanic lithologies were generated under a transitional, orogenic to anorogenic regime, those carrying a predominant arc-related signature (*i.e.*, LO lamprophyre, VR and TM dolerites) are possibly older, whereas the ones denoting a more post-orogenic nature (*i.e.*, Penafiel dolerite, Gonçalo samples, VNFC microgabbro) might be slightly younger.

6. Discussion and Conclusions

Petrographically and chemically, there are no arguments implying that the VNFC microgabbro, Penafiel dolerite, and Gonçalo specimens were influenced by crustal contamination. The prior observation is conformable with the multielement spidergrams (Figura 2), considering the positive Nb and Ta anomalies, as well as the lack of a positive Pb anomaly (*e.g.*, Kirstein *et al.*, 2006; Ma *et al.*, 2014; Soder and Romer, 2018; Orejana *et al.*, 2020). By contrast, the spidergrams for the LO lamprophyre and VR plus TM dolerites reveal an overall LILE and LREE enrichment in regard to the HFSE and HREE, respectively, well-marked negative Nb and Ta anomalies, as well as strong positive Pb anomalies. These features are related to crustal contamination

Table 1. Lithogeochemistry of mafic subvolcanic rocks from northern Portugal. Major elements (SiO2 and K2O) are in weight percent (wt.%), trace elements (Ba, Sr, Sn, W, REE) are in parts per million (ppm), and the A/CNK and ASI ratios are in molar proportion;

Tabela 1. Litogeoquímica de rochas máficas subvulcânicas do norte de Portugal. Elementos maiores (SiO2 e K2O) em peso percentual (wt.%), elementos traço (Ba, Sr, Sn, W, REE) em partes por milhão (ppm), e as razões A/CNK e ASI foram calculadas como proporções molares. Por favor, formatar os 2 em SiO2 e K2O como inferiores à linha.

Samples	Lithology	Locality	SiO_2	K_2O	K_2O/Na_2O	A/CNK	ASI	Ba	Sr	Sn	W	ΣREE
ThetaLO1	Lamprophyre	Lamas de Olo	52.35	7.10	11.83	0.99	1.12	4755	1235	187	50	836.93
ThetaLO2	Lamprophyre	Lamas de Olo	54.32	7.22	16.04	1.03	1.16	4313	1300	103	25	658.23
ThetaLO3	Lamprophyre	Lamas de Olo	54.21	7.57	21.03	1.09	1.24	4465	1355	109	21	733.68
VNFC4	Microgabbro	Vila Nova de Foz Côa	43.85	1.28	0.65	0.67	0.68	326	469	1	1	99.38
VRD1	Dolerite	Vila Real	57.43	2.82	0.91	1.00	1.01	600	530	2	< 1	159.76
VRD2	Dolerite	Vila Real	57.97	3.06	1.00	1.01	1.02	646	529	2	4	171.55
VRD3	Dolerite	Vila Real	58.11	2.35	0.71	1.03	1.04	663	538	2	< 1	168.63
DP	Dolerite	Penafiel	47.03	0.52	0.35	0.83	0.86	151	206	2	< 1	157.94
TMD	Dolerite	Torre de Moncorvo	63.88	5.53	2.25	1.11	1.13	276	216	4	15	101.62
TME	Dolerite	Torre de Moncorvo	57.23	2.89	2.54	1.40	1.41	176	132	2	4	74.41
TMF	Dolerite	Torre de Moncorvo	51.43	2.41	1.01	1.05	1.06	292	253	2	< 1	101.11
TMG	Dolerite	Torre de Moncorvo	52.10	1.76	0.63	0.96	0.97	352	342	1	< 1	160.25
TMH	Dolerite	Torre de Moncorvo	53.65	1.34	0.45	0.88	0.89	350	345	1	1	131.18
TMI	Dolerite	Torre de Moncorvo	53.80	2.94	1.16	0.96	0.97	387	459	1	< 1	164.79
TMI2	Dolerite	Torre de Moncorvo	53.58	3.02	1.20	0.92	0.94	390	449	2	2	160.82
TMJ	Dolerite	Torre de Moncorvo	52.87	1.27	0.48	0.85	0.86	284	486	2	1	100.12
TMJ2	Dolerite	Torre de Moncorvo	54.08	3.06	1.24	0.93	0.94	388	442	2	1	159.98
TMT	Dolerite	Torre de Moncorvo	55.91	3.03	9.77	2.10	2.14	155	29	1	< 1	58.40
BSG	Alkali basalt	Gonçalo (Guarda)	45.33	1.06	0.28	0.82	0.84	229	499	3	3	156.46
BSF	Alkali basalt	Gonçalo (Guarda)	47.43	2.85	0.78	0.82	0.86	343	570	3	2	172.21

and/or subduction-associated, metasomatic enrichment of the mantle sources (*e.g.*, Ma *et al*., 2014). Nonetheless, even for these lithologies, there is ample evidence against the occurrence of contamination, including: (i) the remarkable REE contents of the LO lamprophyre; (ii) the uncorrelated Nb/La and Nb/Th ratios; (iii) the individual values for the Ce/Pb ratio which are significantly distinct compared to those characterizing the continental crust (3.2–3.9) (Taylor and McLennan, 1995); (iv) the negative correlation between Nb/La and La/Sm (in the Vila Real and Torre de Moncorvo cases); (v) the lack of correlation between #Mg and Th/La, #Mg and Sm/Nd, as well as #Mg and Nb/La; and (vi) the uncorrelated SiO_2 concentrations and Rb/Sr ratio (Figura 3). As such, contamination is unlikely to have exerted any meaningful influence on the whole-rock geochemistry of the VR and TM dolerites. However, the occurrence of this phenomenon in the Lamas de Olo case cannot be completely cast aside due to the presence of quartz xenocrysts (Bea *et al*., 1999). Despite the relatively unevolved nature of the VNFC microgabbro, none of the mafic hypabyssal lithotypes is geochemically primitive, attending to the criteria of Frey *et al*. (1978) and Wilson (1989). The prior contemplation implies that crystal fractionation has played either a minor or more meaningful role on the petrogenetic evolution of each subvolcanic specimen.

Several geochemical features of the LO lamprophyre and VR plus TM dolerites, such as the values for the Nb/La ratio (0.15–0.32), suggest that these rocks were generated from subduction-modified lithospheric sources (Bayat and Torabi, 2011). Since the lamprophyre exhibits substantial REE contents and high values for the Rb/Sr ratio (0.29–0.44), melting of the respective source is likely to have occurred shortly after the subduction-related metasomatic event (Liu *et al*., 2020). Metasomatism of the mantle sources for the VR and TM dolerites was presumably dominantly caused by (carbonate-rich) fluids released from dehydration of the subducting plate (Figura 4). Contrastingly, pelagic sediments and the melts formed from their partial melting were, probably, mostly responsible for the metasomatism of the LO lamprophyre source. On the other hand, the VNFC microgabbro and Gonçalo samples (Nb/La = 1.47–1.53) possibly derived from OIB-like, asthenospheric sources, whereas the petrogenesis of the Penafiel dolerite (whose composition displays OIB and E-MORB-like signatures) is presumably associated with both lithospheric and asthenospheric contributions (Nb/La = 0.73).

The sources of the LO lamprophyre, Penafiel dolerite, and Gonçalo specimens were probably situated in the garnet stability field (Dy/Yb = 2.53–3.58), while the sources of the VNFC microgabbro and VR plus TM dolerites might have been located between the garnet and spinel stability fields (Dy/Yb = 1.42–2.39). Furthermore, the melts from which the LO lamprophyre and Gonçalo dyke crystallized possibly resulted from low-degree batch melting (between < 0.1 to 5%) of a garnet-bearing peridotite (Figura 5). For the remaining lithologies, the presence of residual spinel and the source melting degrees (1 to 10%) are implied to have been much higher.

Acknowledgments

This work is supported by national funding awarded by FCT – Foundation for Science and Technology, I.P., projects UIDB/04683/2020 (https://doi.org/10.54499/UIDB/04683/2020) and UIDP/04683/2020 (https://doi.org/10.54499/UIDP/04683/2020). The main author is also financially supported by FCT through an individual Ph.D. grant (reference SFRH/BD/138818/2018).

References

Alici Şen, P., Temel, A., Gourgaud, A., 2004. Petrogenetic modelling of Quaternary post-collisional volcanism: a case study of central and eastern Anatolia. *Geological Magazine,* **141**:81-98. https://doi.org/10.1017/S0016756803008550.

Bayat, F., Torabi, G., 2011. Alkaline lamprophyric province of Central Iran. *Island Arc*, **20**:386-400. https://doi.org/10.1111/j.1440-1738.2011.00776.x.

Bea, F., Montero, P., Molina, J. F., 1999. Mafic Precursors, Peraluminous Granitoids, and Late Lamprophyres in the Avila Batholith: A Model for the Generation of Variscan Batholiths in Iberia. *The Journal of Geology*, **107**:399-419. https://doi.org/10.1086/314356.

Caroff, M., Barrat, J.-A., Le Gall, B., 2021. Kersantites and associated intrusives from the type locality (Kersanton), Variscan Belt of Western Armorica (France). *Gondwana Research*, **98**:46-62. https://doi.org/10.1016/j.gr.2021.06.004.

Ferreira, M.P., Macedo, A.R., 1979. Atividade magmática durante o Mesozóico: 1 – Achega para a datação K-Ar das rochas filonianas básicas intrusivas na Zona Centro Ibérica (Portugal). *Memórias e Notícias, Publicações do Museu e Laboratório Mineralógico e Geológico da Universidade de Coimbra,* **87**:29-49.

Ferreira, N., Iglésias, M., Noronha, F., Ribeiro, A., Ribeiro, M. L., 1987. Granitóides da Zona Centro Ibérica e seu enquadramento geodinâmico. In: Bea, F., Carnicero, A., Gonzalo, J.C., López Plaza, M., Rodriguez Alonso, M.D. (Eds.), *Geologia de los Granitoides e Rocas Asociadas del Macizo Hespérico*, Editorial Rueda, Madrid, 37-51.

Frey, F. A., Green, D. H., Roy, S. D., 1978. Integrated models of basalt petrogenesis: a study of quartz tholeiites to olivine melilitites from south eastern Australia utilizing geochemical and experimental petrological data. *Journal of Petrology*, **19**:463-513. https://doi.org/10.1093/petrology/19.3.463.

Kirstein, L. A., Davies, G.R., Heeremans, M., 2006. The petrogenesis of Carboniferous-Permian dyke and sill intrusions across northern Europe. *Contributions to Mineralogy and Petrology*, **152**:721-742. https://doi.org/10.1007/s00410-006-0129-9.

LaFlèche, M. R., Camiré, G., Jenner, G.A., 1998. Geochemistry of post-Acadian, Carboniferous continental intraplate basalts from the Maritimes Basin, Magdalen Islands, Québec, Canada. *Chemical Geology*, **148**:115-136. https://doi.org/10.1016/S0009-2541(98)00002-3.

Liu, B., Wu, J.H., Li, H., Wu, Q.H., Evans, N.J., Kong, H., Xi, X.S., 2020. Geochronology, geochemistry and petrogenesis of the Dengfuxian lamprophyres: Implications for the early Cretaceous tectonic evolution of the South China Block. *Geochemistry*, **80**:125598. https://doi.org/10.1016/j.chemer.2020.125598.

Ma, L., Jiang, S.Y., Hofmann, A.W., Dai, B.Z., Hou, M.L., Zhao, K.D., Chen, L.H., Li, J.W., Jiang, Y.H., 2014. Lithospheric and asthenospheric sources of lamprophyres in the Jiaodong Peninsula: a consequence of rapid lithospheric thinning beneath the North China Craton? *Geochimica et Cosmochimica Acta*, **124**:250-271. https://doi.org/10.1016/j.gca.2013.09.035.

McDonough, W. F., 1990. Constraints on the composition of the continental lithospheric mantle. *Earth and Planetary Science Letters*, **101**:1-18. https://doi.org/10.1016/0012-821X(90)90119-I.

McDonough, W. F., Sun, S.S., 1995. The Composition of the Earth. *Chemical Geology*, **120**, 223-253. https://doi.org/10.1016/0009-2541(94)00140-4.

Oliveira, A., Martins, H. C. B., Sant'Ovaia, H., 2022. Permo-Carboniferous hypabyssal magmatism in northern Portugal: the case of the Lamas de Olo microgranite and lamprophyre dykes. *Journal of Iberian Geology*, **48**:1-28. https://doi.org/10.1007/s41513-021-00179-8.

Orejana, D., Villaseca, C., Billström, K., Paterson, B.A., 2008. Petrogenesis of Permian alkaline lamprophyres and diabases from the Spanish Central System and their geodynamic context within western Europe. *Contributions to Mineralogy and Petrology*, **156**, 477-500. https://doi.org/10.1007/s00410-008-0297-x.

Orejana, D., Villaseca, C., Kristoffersen, M., 2020. Geochemistry and geochronology of mafic rocks from the Spanish Central System: Constraints on the mantle evolution beneath central Spain. *Geoscience Frontiers*, **11**: 1651-1667. https://doi.org/10.1016/j.gsf.2020.01.002.

Perini, G., Cebria, J.M., Lopez-Ruiz, J., Doblas, M., 2004. Carboniferous-Permian mafic magmatism in the Variscan belt of Spain and France: implications for mantle sources. *Geological Society, London, Special Publications*, **223**:415-438. https://doi.org/10.1144/GSL.SP.2004.223.01.18.

Ramos, V., Noronha, F., 2019. Geoquímica de um filão de rochas básicas alcalinas de Gonçalo (Guarda). *Livro de Atas do XII Congresso Ibérico de Geoquímica e X Semana de Geoquímica*, Évora, Portugal, 137-140.

Rock, N. M. S. (1991). *Lamprophyres*. Blackie, Glasgow.

Sen, G., Leeman, W. P., 1991. Iron-rich lherzolitic xenoliths from Oahu: origin and implications for Hawaiian magma sources. *Earth and Planetary Science Letters*, **102** (1):45-57. https://doi.org/10.1016/0012-821X(91)90016-B.

Shaw, D. M., 1970. Trace element fractionation during anatexis. *Geochimica et Cosmochimica Acta*, **34**:237-243. https://doi.org/10.1016/0016-7037(70)90009-8.

Soder, C. G., Romer, R. L., 2018. Post-collisional Potassic–Ultrapotassic Magmatism of the Variscan Orogen: Implications for Mantle Metasomatism during Continental Subduction. *Journal of Petrology*, **59**: 1007-1034. https://doi.org/10.1093/petrology/egy053.

Taylor, S. R., McLennan, S. M., 1995. The geochemical evolution of the continental crust. *Reviews of Geophysics*, **33**:241-265. https://doi.org/10.1029/95RG00262.

Villaseca, C., Orejana, D., Higueras, P., Pérez-Soba, C., Serrano, J.G., Lorenzo, S., 2022. The evolution of the subcontinental mantle beneath the Central Iberian Zone: Geochemical tracking of its mafic magmatism from the Neoproterozoic to the Cenozoic. *Earth-Science Reviews*, **228**:103997. https://doi.org/10.1016/j.earscirev.2022.103997.

Wilson, M., 1989. *Igneous Petrogenesis*. Springer, Dordrecht. https://doi.org/10.1007/978-1-4020-6788-4.